Eur. Phys. J. B **13**, 679–683 (2000)

THE EUROPEAN PHYSICAL JOURNAL B

EDP Sciences

Ab initio study of phonons in the rutile structure of SnO_2 under pressure

K. Parlinski[a] and Y. Kawazoe

Institute for Materials Research, Tohoku University, 2-1-1 Katahira, Sendai 980-8577, Japan

Received 18 July 1999

Abstract. Using the local-density approximation, calculating the Hellmann-Feynman forces and applying the direct method, the phonon dispersion relations for the rutile-like structure of crystalline SnO_2 have been derived for the first time. The phonon frequencies at the Γ point agree very well with Raman and infrared data and other phenomenological model calculations. The LO/TO splitting is estimated by calculating phonons from an elongated supercell. The computations under pressure reveal a soft mode of B_{1g} symmetry which leads to a ferroelastic phase transition. The pressure-dependence of the lattice constants and the Grüneisen parameters of the modes are calculated.

PACS. 63.20.-e Phonons in crystal lattices – 71.15.Mb Density functional theory, local density approximation – 62.50.+p High-pressure and shock-wave effects in solids and liquids

1 Introduction

There is a great degree of interest in the high-pressure phases of silica SiO_2 [1,2], in particular in rutile-type structure stishovite, due to the possible geophysical repercussions. The stishovite transforms to an orthorhombic $CaCl_2$-type phase around 100 GPa. The existence of post-stishovite high-pressure phases of silica would be of substantial geophysical importance as free silica can coexist with $(Mg, Fe)O$ in the lowermost mantle [3]. An appropriate model compound for stishovite is the rutile-type SnO_2, since in SnO_2 a similar phase transition to $CaCl_2$-type phase occurs at an order of magnitude lower pressure. This makes SnO_2 much more accessible to experiment. In addition SnO_2 semiconducting properties are extensively used in thin films to provide simultaneously an electrically conducting and visibly transparent layer.

At ambient pressure SnO_2 has a rutile structure with $P4_2/mnn$ (D_{4h}^{14}) symmetry and 6 atoms in the unit cell [4,5]. Above 11.8 GPa under hydrostatic pressure the rutile-structure SnO_2 undergoes a second-order phase transition to a $CaCl_2$-type phase with Pnnm (D_{2h}^{12}) symmetry. At ambient pressure the Raman and infrared spectra have been measured for a single crystal of SnO_2 [6] and 11 mode frequencies out of 15 have been determined. Other measurements [7] carried out under pressure up to 0.42 GPa delivered four Raman-active phonon frequencies and the estimate of the Grüneisen parameters.

The lattice dynamics of rutile-type structure SnO_2 has been considered several times within phenomenological approaches. A rigid-ion model with short range central axially symmetric forces and long range Coulomb forces, fitted to experimental frequencies, has been considered in reference [6]. The rigid-ion model was extended to first and second nearest neighbour central and oxygen-tin-oxygen bending forces, and the zone-center Γ point modes were calculated [8]. Then, it proved that the shell model satisfactory reproduces the TiO_2 phonon dispersion curves measured by coherent inelastic neutron scattering [9]. The shell model for SnO_2 was obtained by slightly readjusting the TiO_2 parameters in such a way that the best fit of the measured infrared and Raman frequencies could be achieved [10]. Later, the shell model was again used [11] in relation with the analysis of the temperature dependence of the linewidth of A_{1g} mode in the Raman spectrum of SnO_2.

To deal with *ab initio* lattice dynamics two approaches are currently in use: the linear response [12], and the direct method. In the linear response method the dynamical matrix is obtained from the modification of the electronic density, *via* the inverse dielectric matrix, resulting from the phonon displacements of atoms. The dynamical matrix can be determined at any wave vector in the Brillouin zone, with a computational effort comparable to a ground-state optimization. Only linear effects, such as harmonic phonons, are accessible to this technique. The direct method approach [13–17] is based on the *ab initio* pseudopotential plane-wave total energy calculations, which allows the study of both linear and nonlinear effects. The computer codes deal with a supercell which allows explicit account of any perturbation, including

[a] On leave from the Institute of Nuclear Physics, ul. Radzikowskiego 152, 31-342 Cracow, Poland
e-mail: Krzysztof.Parlinski@ifj.edu.pl

Table 1. Zero-pressure structural parameters of rutile-type SnO_2.

	a [Å]	c [Å]	x
Present calc.	4.6809	3.1790	0.3056
X-rays [4]	4.7367(1)	3.1855(1)	0.3070(4)
Neutrons [5]	4.7374(1)	3.1864(1)	0.3056(1)

the calculation of the Hellmann-Feynman forces generated by a displaced atom. In the direct method these forces are used to derive the force constants, dynamical matrix and phonon frequencies.

In this note we present the *ab initio* calculations of the structure and lattice dynamics of rutile-type SnO_2. Such calculations are even more important, since neither the *ab initio* study has been made, nor the phonon dispersion relations have been measured. Moreover, in the rutile-like phase of GeO_2 the B_{1g} mode has been shown to be soft [18]. The present *ab initio* calculations are undertaken to search for similar B_{1g} pressure-dependent soft mode in SnO_2. The first-principle pseudopotential calculations within the local-density approximation, but for another rutile-like structure, namely for stishovite SiO_2, have been carried on in reference [19]. There only the Γ point transverse optic modes of SiO_2 were determined as functions of pressure. It was also shown that the phase transition from rutile-like to $CaCl_2$-type structure is associated with an elastic instability of B_{1g} symmetry.

2 Method

The *ab initio* calculations for SnO_2 are performed using the pseudopotential method within the local-density approximation (LDA) as implemented in VASP package [20,21], and with the ultrasoft pseudopotentials provided with VASP. The pseudopotentials for Sn and O atoms are representing $s^2p^2f^0$, and $s^2p^4d^0$ electron configurations, respectively. We have used supercells of $1\times1\times1$, $2\times2\times2$, and $1\times1\times8$ sizes with 6, 48 and 48 atoms, respectively. With the $1\times1\times1$ supercell the pressure dependence of phonon mode frequencies at the Γ point are calculated. The $2\times2\times2$ supercell is used to derive phonon dispersion relations. The $1\times1\times8$ supercell allows us to estimate the longitudinal optical A_{2u}(LO) mode frequency. A plane-wave basis set with 400 eV cutoff is used to expand the electronic wave functions at special k points generated by $4\times4\times4$, $2\times2\times2$, $4\times4\times1$, Monkhurst-Pack k meshes, for mentioned supercells, respectively. The unit cell parameters of the optimized zero-pressure rutile structure of SnO_2 are shown in Table 1. They are in usual agreement with experiments [4,5].

The phonons are determined by the direct method [22] using optimized $2\times2\times2$ supercell. For that the Hellmann-Feynman forces are computed for four independent displacements, two along x and two along z for Sn and O atoms as required by the tetragonal symmetry. The displacement amplitude is 0.5% of the lattice constant in a given direction. To minimize anharmonic effects, we make positive and negative displacements about equilibrium positions. All displaced configurations generate

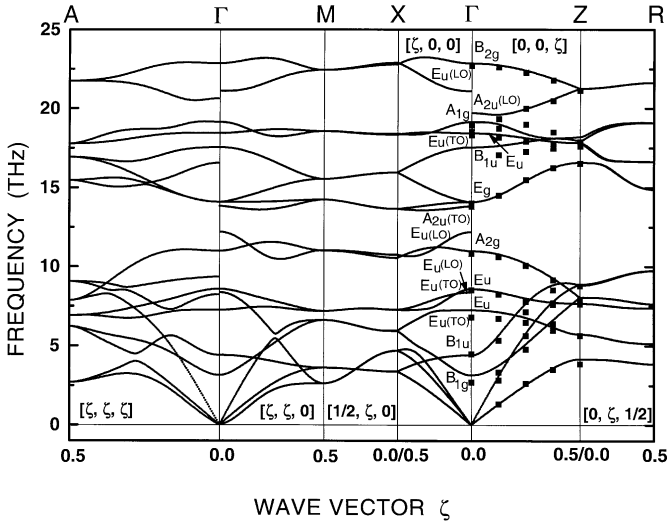

Fig. 1. Phonon dispersion relations of the rutile-like phase of SnO_2 calculated from $2\times2\times2$ supercell. Squares denote phonon frequencies found from $1\times1\times8$ supercell.

$4\times3\times48=576$ components of Hellmann-Feynman forces. Next, the symmetry of the force constants, following from $P4_2/mnn$ space group, is established and 165 independent parameters of so-called cummulant force constants [17,23], belonging to 34 coordination shells, are fitted to the collected Hellmann-Feynman forces by the singular value decomposition method, which simultaneously provides the least-square solution.

The magnitude of the force constants diminishes with distance between the atoms involved. The largest ones are the on-site force constants (zero distance). At 3.179 Å, which is the shortest distance from the central atom of the supercell to the surface along $[0,0,1]$ direction, the largest element of the force constant is about 15 times smaller than the on-site force constants. At 4.737 Å along $[1,0,0]$ direction this factor increases to 20 times, while at the corner along $[1,1,1]$ direction the force constants diminish by a factor of about 300.

The force constants are used to construct the dynamical matrix, to diagonalize it and to find phonon frequencies. According to the direct method the tetragonal $2\times2\times2$ supercell provides correct phonon frequencies, independent of the range of interaction, at the Γ $(0,0,0)$ (except for longitudinal optic (LO) infrared active modes), $X(\frac{1}{2},0,0)$, $Z(0,0,\frac{1}{2})$, $M(\frac{1}{2},\frac{1}{2},0)$, $R(\frac{1}{2},0,\frac{1}{2})$ and $A(\frac{1}{2},\frac{1}{2},\frac{1}{2})$ special points of the simple tetragonal Brillouin zone. Since the magnitude of the force constants decreases out relatively fast within the supercell range, the phonon branches, being an interpolation between special points Γ, X, Z, M, R, A, should be relatively well reproduced.

3 Phonon dispersion relations

The calculated dispersion curves at zero pressure are displayed in Figure 1. The phonon frequencies at the Γ point are compared in Table 2 with experimental data and phenomenological model calculations, and the agreement is very good. A somewhat lower accuracy of A_{2u}(LO),

Table 2. Comparison of the mode frequencies at the Γ point for SnO_2. Frequencies are in THz.

Mode	Present calc.	Expt. [6]	Expt. [7]	Calc. [6]	Calc. [8]	Calc. [10]	Calc. [11]
A_{1g}	19.13	19.13	19.10	19.37	18.84	20.30	19.17
A_{2g}	10.98	-	-	11.95	14.64	-	-
B_{1g}	3.14	-	3.63	3.00	3.68	5.52	3.80
B_{2g}	22.84	23.45	23.41	22.54	23.03	23.35	22.81
E_g	14.08	14.27	14.27	13.22	14.93	14.27	13.53
$B_{1u}^{(1)}$	4.40	-	-	4.20	4.48	-	-
$B_{1u}^{(2)}$	17.54	-	-	15.14	18.09	-	-
A_{2u}(TO)	13.82	14.30	-	15.35	14.30	14.00	15.39
$E_u^{(1)}$(TO)	7.24	7.32	-	7.08	6.98	7.08	7.43
$E_u^{(2)}$(TO)	8.57	8.78	-	8.90	9.14	9.32	10.14
$E_u^{(3)}$(TO)	18.43	18.53	-	19.52	19.41	16.82	19.82
A_{2u}(LO)	19.70	21.13	-	20.60	21.09	21.29	19.68
$E_u^{(1)}$(LO)	8.36	8.27	-	8.03	7.40	8.69	7.43
$E_u^{(2)}$(LO)	12.18	10.97	-	11.30	14.32	12.11	12.77
$E_u^{(3)}$(LO)	21.09	23.08	-	22.48	22.12	21.20	19.82

Table 3. Calculated mode frequencies at the X, M, Z, R, and A points in the Brillouin zone. All modes are doubly degenerate. Frequencies are in THz.

X	M	Z	R	A
3.37	2.62	4.16	3.85	2.68
4.68	3.60	5.72	5.13	6.21
5.93	6.61	7.67	7.37	6.89
7.26	7.18	8.04	7.63	7.85
10.54	11.00	8.80	9.73	9.05
13.64	14.22	16.58	14.87	14.45
15.94	15.54	17.82	16.23	16.92
18.34	18.56	17.91	19.08	17.77
22.77	22.41	21.24	21.62	21.73

$E_u^{(2)}$(LO) $E_u^{(3)}$(LO) might be caused by the method of estimating the LO/TO splitting described below. Nevertheless, the overall agreement of the calculated frequencies (4.2%) at Γ point with experimental data [6,7] is of the same order as those obtained by the rigid-ions (4.8%) [6], (5.0%) [8], and shell model calculations (7.0%) [10] and (7.9%) [11]. In Table 3 are collected phonon frequencies at all high-symmetry points in the Brillouin zone, namely at X, Z, M, R, A.

The interaction of tin and oxygen ions with the macroscopic electric field leads to LO/TO splitting of infrared active modes. The direct method with a $2\times2\times2$ supercell allows us to calculate only TO modes. The LO modes can be extracted from the elongated supercell using the direct method as well [24]. For that we build a $1\times1\times8$ supercell elongated in the z-direction with 48 atoms, calculate the Hellmann-Feynman forces for x and z displacements of Sn and O atoms, and derive the dispersion curves along the Γ–Z direction. This supercell provides correct phonons at four wave vectors: $(0,0,\frac{1}{8})$, $(0,0,\frac{1}{4})$, $(0,0,\frac{3}{8})$, Z $(0,0,\frac{1}{2})$. They are shown in Figure 1. We use these four points to extrapolate the LO branch to the Γ point, where we find the frequency of the A_{2u}(LO) mode to be 19.70 THz.

The LO modes at Γ point depend on the non-analytical term [25] which in turn depends on effective charge tensors $\mathbf{Z}^*$ and the electronic part of the dielectric constant ϵ_∞. The non-analytical term has to be added to the dynamical matrix derived by the direct method. We assume that the effective charge tensor can be approximated by the point charge Z^*. From the frequency 19.70 THz of the A_{2u}(LO) mode we find the values of the effective charges as $Z^*(\mathrm{Sn})/\sqrt{\epsilon_\infty} = 1.98$ and $Z^*(\mathrm{O})/\sqrt{\epsilon_\infty} = -0.99$. In reference [6] the values 1.96 and -0.98 are given, respectively, which are found by fitting the rigid ion model to experimental data. Our point effective charges are used to compute frequencies of E_u(LO) modes and the results are shown in Figure 1 and given in Table 2.

4 Phonon modes under pressure

The *ab initio* calculations are carried out also at high pressures. The $1\times1\times1$ supercell of SnO_2 is optimized, and the phonons at the Γ point are calculated at several pressures up to 10.0 GPa. In this interval the lattice parameters, the unit cell ratio c/a and volume V change linearly. These quantities are shown in Figure 2 and they perfectly agree with the experimental data of reference [4] taken at the compression and decompression. In particular, the present calculations and data of reference [4] show that c/a ratio increases with increasing pressure, contrary to measurements of reference [7], which predicts that c/a ratio should decrease. Linear pressure dependence of almost all phonon modes is found, and hence the Grüneisen parameters $\nu_i = -(\partial \ln\omega_i/\partial \ln V)\ |_{T=0}$ are computed and listed in Table 4, and compared with experimental data [7]. Generally, the mode frequency increases with pressure, except for slight decrease of $E_u^{(1)}$(TO) mode, and real softening of B_{1g} mode (Fig. 3). The essential part of the phonon dispersion relations along Γ–M direction, which includes the B_{1g} soft mode and the acoustic modes,

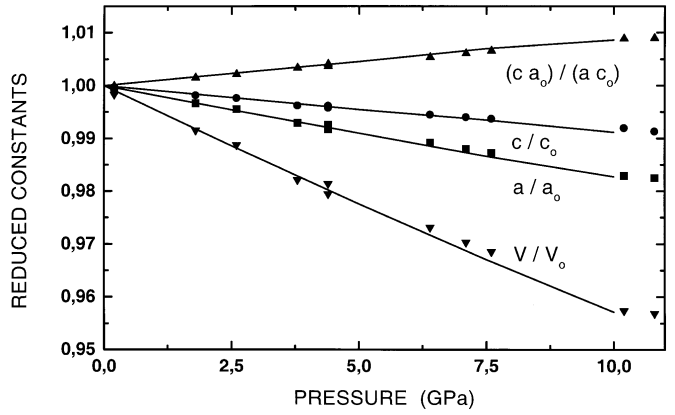

Fig. 2. Pressure dependence (lines) of a and c tetragonal lattice constants, c/a ratio and V unit cell volume of rutile-like structure of SnO_2. Experimental points are taken from reference [2].

Table 4. Grüneisen parameters ν_i of the modes.

Mode	Present calc.	Expt.[7]	Mode	Present calc.
A_{1g}	1.33	3.64	$B_{1u}^{(2)}$	1.56
A_{2g}	0.63	-	A_{2u}(TO)	1.32
B_{1g}	−14.17	−10.44	$E_u^{(1)}$(TO)	−0.61
B_{2g}	1.49	2.58	$E_u^{(2)}$(TO)	1.14
E_g	1.29	3.20	$E_u^{(3)}$(TO)	1.91
$B_{1u}^{(2)}$	0.26	-	-	-

is shown in Figure 3a for two pressures. Beyond the Γ point the B_{1g} soft mode branch interacts with the transverse acoustic (TA) mode and causes that part of the TA branch close to Γ point becomes imaginary (negative in Fig. 3a). The minimum of the TA branch occurs along the Γ–M direction. This destabilizes the tetragonal crystal and leads, through the ferroelastic phase transition, to the orthorhombic $CaCl_2$-type phase. The instability of the TA mode occurs around 7.0 GPa which is lower than the value of 11.8 GPa found experimentally at ambient temperature.

5 Conclusions

In conclusion we have calculated the *ab initio* lattice dynamics of rutile-type structure of SnO_2. The LO mode was found from extrapolation of the $\mathbf{k} \to 0$ of the optic phonon branch restored with elongated supercell. Calculations under pressure revealed a soft mode of B_{1g} symmetry which leads to the ferroelastic phase transition accompanied by softening of the transverse acoustic mode propagating along the $[1, 1, 0]$ direction.

We thank K. Esfarjani, K. Ohno, and M.H.F. Sluiter for valuable comments. One of us (K.P.) would like to express his thanks to the staff of the Laboratory of Materials Design by Computer Simulation, Institute of Materials Research, Tohoku University, for their great hospitality and assistance during his stay. This work was partially supported by the State Committee of Scientific Research (KBN), grant No. 2 PO3B 004 14.

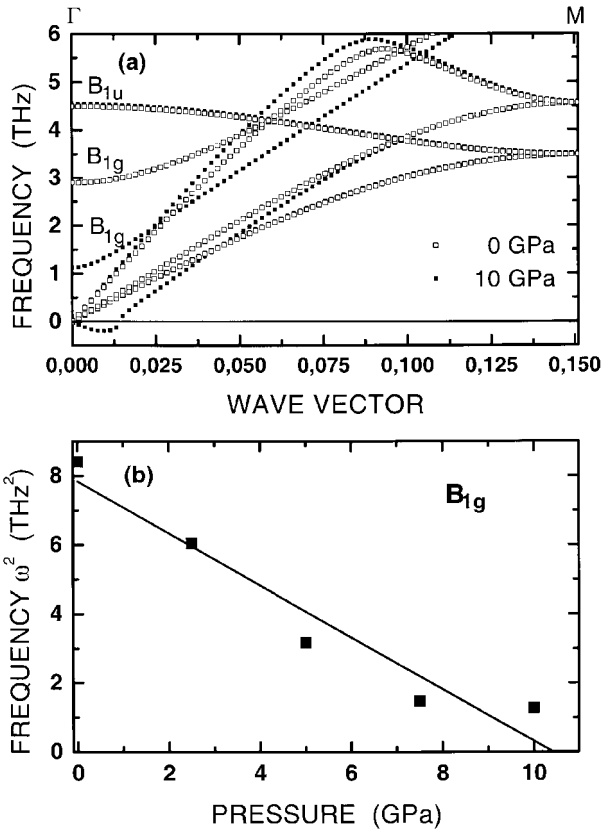

Fig. 3. (a) Phonon dispersion relations along Γ–M direction at pressures of 0 GPa and 10 GPa for the rutile-like phase of SnO_2 showing the softening of the B_{1g} mode and softening of the transverse acoustic branch. (b) Pressure-dependence of the B_{1g} soft mode.

References

1. D.M. Teter, R.J. Hemley, G. Kresse, J. Hafner, Phys. Rev. Lett. **80**, 2145 (1998).
2. Th. Demuth, Y. Jeanvoine, J. Hafner, J.G. Ángyán, J. Phys. Cond. Matter **11**, 3833 (1999).
3. E. Knittle, R. Jeanloz, Science **251**, 1438 (1991).
4. J. Haines, J.M. Légar, Phys. Rev. B **55**, 11 444 (1997).
5. A.A. Bolzan, C. Fong, B.J. Kennedy, C.J. Howard, Acta Cryst. B **58**, 373 (1997).
6. R.S. Katiyar, P. Dawson, M.M. Hargreave, G.R. Wilkinson, J. Phys. C **4**, 2421 (1971).
7. P.S. Peercy, B. Morosin, Phys. Rev. **7**, 2779 (1973).
8. M.E. Striefler, G.R. Barsch, Phys. Stat. Sol. B **67**, 143 (1975).
9. J. Heines, J.M. Légar, O. Schulte, Science B **271**, 629 (1996).
10. F. Gervais, W. Kress, Phys. Rev. B **31**, 4809 (1985).
11. T. Sato, T. Asari, J. Phys. Soc. Jpn **64**, 1193 (1995).
12. S. Baroni, P. Giannozzi, A. Testa, Phys. Rev. Lett. **58**, 1861 (1987).

13. R. Resta, K. Kunc, Phys. Rev. B **34**, 7146 (1986).
14. W. Frank, C. Elsässer, M. Fähnle, Phys. Rev. Lett. **74**, 1791 (1995).
15. G. Kresse, J. Furthmüller, J. Hafner, Europhys. Lett. **32**, 729 (1995).
16. G.J. Ackland, M.C. Warren, S.J. Clark, J. Phys.-Cond. Matter **9**, 7861 (1997).
17. K. Parlinski, Z.Q. Li, Y. Kawazoe, Phys. Rev. Lett. **78**, 4063 (1997).
18. J. Haines, J.M. Légar, C. Chateau, R. Bini, L. Ulivi, Phys. Rev. B **58**, 1 (1998).
19. B.B. Karki, M.C. Warren, L. Stixrude, G.J. Ackland, J. Crain, Phys. Rev. B **55**, 3465 (1997).
20. G. Kresse, J. Hafner, Phys. Rev. B **47**, 558 (1993); *ibid* **49**, 14 251 (1994).
21. G. Kresse, J. Furhmüller, Software VASP, Vienna (1999); Phys. Rev. B **54**, 11 169 (1996); Comput. Mat. Science **6**, 15 (1996).
22. K. Parlinski, Software PHONON (1999).
23. K. Parlinski, *Neutrons and Numerical Methods - N_2M*, API Conf. Proc. 479, edited by M.R. Johnson, G.J. Kearley, H.G. Büttner (Woodbury, New York, 1999), p. 121.
24. K. Parlinski, J. Łażewski, Y. Kawazoe, J. Phys. Chem. Solids **61**, 87 (1999).
25. R.M. Pick, M.H. Cohen, R.M. Martin, Phys. Rev. B **1**, 910 (1970); A.A. Maradudin, Elements of the Theory of Lattice Dynamics, in *Dynamical Properties of Solids*, edited by G.K. Horton, A.A. Maradudin, (North-Holland Publishing Company, Amsterdam, 1974), Vol. 1, p. 3.